NASA Contractor Report 168221

Comparisons of Rational Engineering Correlations of Thermophoretically-Augmented Particle Mass Transfer with STAN5-Predictions for Developing Boundary Layers

Süleyman A. Gökoğlu

Analex Corporation
Cleveland, Ohio

and

Daniel E. Rosner

Yale University
New Haven, Connecticut

January 1984

COMPARISONS OF RATIONAL ENGINEERING CORRELATIONS OF

THERMOPHORETICALLY-AUGMENTED PARTICLE MASS TRANSFER

WITH STAN5-PREDICTIONS FOR DEVELOPING BOUNDARY LAYERS[1]

Süleyman A. Gökoğlu[2]
Analex Corporation
Cleveland, Ohio 44135

and

Daniel E. Rosner[3]
Yale University
Chemical Engineering Department
New Haven, Connecticut 06520

SUMMARY

Fouling (and corrosion) of gas turbine (GT) blading often results from the deposition of materials derived from inorganic impurities in the fuel and/or ingested air. When the depositing material is in the form of a sub-micron "aerosol" (dust or mist) it has been found that the rates of deposition on cooled surfaces can be augmented by some 100-1000-fold via the mechanism of thermophoresis (particle migration down a temperature gradient). For this reason, in earlier papers we reported the development of rational, yet simple, engineering correlations of thermophoretically-augmented particle transport across both laminar boundary layers (LBLs) and turbulent boundary layers (TBLs). While developed based on theoretical considerations, and numerical computations of self-similar LBLs and law-of-the-wall (Couette flow-like) TBLs, these mass transfer coefficient (St_m-) correlations, when applied locally, may also prove useful in making engineering mass transfer predictions for more complex geometries, including GT-blades. Pending additional controlled experiments, insight into the local applicability of these correlations can be gained by selected comparisons with numerical predictions for developing BLs. This paper reports on our (a) modification of the code STAN5 to properly include thermophoretic mass transport, and (b) examination of selected test cases of developing BLs which include variable properties, viscous dissipation, transition to turbulence and transpiration cooling. Under conditions representative of current and projected GT operation, local application of our $St_m/St_{m,o}$- correlations evidently provides accurate and economical engineering design predictions, especially for suspended particles characterized by Schmidt numbers outside of the heavy vapor range (say, $Sc > 10$).

E-1991

INTRODUCTION

Accurate predictions of <u>mass</u> transport rates in nonisothermal forced convection systems are now essential to the gas turbine (GT) industry, among other technologies. Recently, a dramatic enhancement in small particle diffusional transport rates due to <u>thermophoresis</u> (particle drift down a temperature gradient) has been predicted for both internally cooledand transpiration-cooled surfaces across both self-similar laminar boundary layers (LBLs) (refs. 1 and 2) and law-of-the-wall <u>turbulent</u> (ref. 3.) boundary layers (TBLs), including viscous dissipation (ref. 4). The magnitude and temperature dependence of this thermophoretic augmentation has been experimentally confirmed for LBL flow of combustion products containing submicron M_gO-particles (ref. 5).

To facilitate engineering predictions, simple rational <u>correlations</u> have recently been developed (refs. 6 and 7). Until now their accuracy and applicability limits have been demonstrated using "exact" numerical calculations for self-similar BLs (refs. 1 and 4). One of our purposes here is to examine their behavior and accuracy in more complex BL-flows, under conditions representative of current and future GT-technology.

The availability of high-speed, large capacity computers has made it possible to examine the reliability of self-similar <u>heat</u> transfer correlations when applied locally to <u>developing</u> BL situations. Indeed, computer codes for both multidimensional laminar and turbulent flows have been developed by exploiting finite-difference techniques (refs. 8 and 9). Recently, with increased interest in GT blade fouling and/or corrosion problems, greater attention is being focused on small particle <u>mass</u> transfer across two-dimensional BL's (ref. 10). To make such predictions we have adapted the two-dimensional BL code STAN5 (ref. 11), which has previously been widely used for gas-side convective <u>heat</u> transfer predictions. This necessitated modifying the program to now include thermal (Soret) diffusion ("thermophoresis" for small particles) in the suspended particle mass conservation (particle-phase "continuity") equation. Toward this end, STAN5 predictions over the suction surface of a typical stator blade are here compared with the predictions of our earlier correlations (refs. 6 and 7) when applied locally to such developing BL situations. Of course, experimental data, both for blade cascades and operational turbines, will be the ultimate arbiter of whether our correlations and/or numerical BL codes (e.g., STAN5) presently and properly include all of the phenomena which dictate mass transport rates in the challenging GT environment.

NOMENCLATURE

B_m	real blowing parameter, eq. (5)
$-B_T$	thermophoretic suction parameter, eq. (6)
c	mass fraction of particles in the local gas mixture
D	Brownian diffusion coefficient of particles
Da	effective Damkohler number, eq. (7)
Le	Lewis number (ratio of particle Brownian diffusivity to host gas heat diffusivity)

$\dot{m}''$	mass flux at station e or w
Ma	Mach number
p	pressure
r	radius (for axisymmetric BL flow)
R_n	nose radius of the turbine blade
S	source; eq. (3)
Sc	Schmidt number (ratio of host gas momentum diffusivity (kinematic viscosity) to particle Brownian (mass) diffusivity)
St_h	Stanton number for heat transfer
St_m	Stanton number for mass transfer, including thermophoresis
$St_{m,o}$	Stanton number for mass transfer without thermophoresis and/or transpiration cooling
T	absolute temperature
T_m	temperature at the outer edge of Brownian diffusion boundary layer
u	fluid velocity in x-direction (parallel to wall)
v	fluid velocity in y-direction (normal to wall)
x	distance along the surface (measured from the forward stagnation point)
y	distance normal to surface
α_T	thermal diffusion factor of the particle/host gas combination
μ	dynamic viscosity of host gas
ρ	density of host gas
ψ	stream function coordinate, $\rho u r = \partial\psi/\partial y$, $\rho v r = -\partial\psi/\partial x$
ω	nondimensional stream function coordinate, $(\psi-\psi_w)/(\psi_e-\psi_w)$

Subscripts:

e	pertaining to the outer edge of the boundary layer
eff	effective
o	pertaining to reservoir conditions (transpiration coolant)
w	pertaining to the surface (wall)
∞	pertaining to gas mixture at upstream "infinity"

Miscellaneous:

BL	boundary layer (L, laminar; T, turbulent)
GT	gas turbine
PDE	partial differential equation
RHS	right hand side

ADDITION OF THERMOPHORESIS TO STAN5 BL CODE

Here we focus only on the suspended particle mass conservation PDE, which must include the thermophoretic flux term. Upon time-averaging, the simultaneous fluctuation of the thermophoretic speed and particle concentration produces a new "correlation" term. But this latter term (which may be called "eddy thermophoresis") is neglected based on arguments given in references 12 and 13. In the same notation as reference 11, the time-averaged particle mass conservation equation for the BL can then be written:

$$\rho u \frac{\partial c}{\partial x} + \rho v \frac{\partial c}{\partial y} = \frac{1}{r} \frac{\partial}{\partial y} \left(r \frac{\mu_{eff}}{Sc_{eff}} \frac{\partial c}{\partial y} \right) + \frac{1}{r} \frac{\partial}{\partial y} \left(\frac{r \rho \alpha_T Dc}{T} \frac{\partial T}{\partial y} \right) \tag{1}$$

where the second term on the RHS of equation (1) is the added thermophoretic flux. Upon introducing the nondimensional stream function as the transverse coordinate (cf. ref. 11) equation (1) becomes:

$$\frac{\partial c}{\partial x} + \left[\frac{r_w \dot{m}''_w + \omega(r_e \dot{m}''_e - r_w \dot{m}''_w)}{(\psi_e - \psi_w)} \cdot \frac{\partial c}{\partial \omega} \right]$$

$$- \frac{\partial}{\partial \omega} \left[\frac{r^2 \rho u \, \mu_{eff}}{(\psi_e - \psi_w)^2 \, Sc_{eff}} \cdot \frac{\partial c}{\partial \omega} \right] = \frac{\partial}{\partial \omega} \left[\frac{r^2 \rho^2 u \alpha_T Dc}{(\psi_e - \psi_w)^2 \, T} \cdot \frac{\partial T}{\partial \omega} \right] \tag{2}$$

In the numerical solution of equation (2) the thermophoretic flux term on the RHS will be treated as a "source" term. Although the source itself is explicitly c-dependent, c-values obtained from the previous (upstream) integration step are used in its evaluation. This simple treatment of the thermophoretic flux term is compatible with numerical approximations already incorporated in STAN5. For flow near the wall, where STAN5 switches to simplified Couette-flow equations (with no streamwise variation of the dependent variable, and constant r), the thermophoretic flux term is included in the particle mass conservation equation, again as the "source" defined by:

$$S \equiv \frac{\partial}{\partial y} \left(\frac{\rho \alpha_T Dc}{T} \frac{\partial T}{\partial y} \right) \tag{3}$$

Based on the procedures outlined in reference 14, new subroutines have been added to STAN5 in order to calculate the suspended particle thermal diffusion factor, α_T, and the Brownian diffusion coefficient, D (as well as the Schmidt number, Sc), including their respective temperature dependencies.

The modification in particle deposition rate due to thermophoresis depends both on particle size (hence Schmidt number) and the ratio of mainstream-to-surface-temperature. Therefore, under typical turbine operating conditions, in order to see an appreciable thermophoretic effect one needs to consider particles heavier than ordinary vapor molecules. However, as is well known, when the particle size increases (enough to cause $Sc \gg 1$), the mass transfer (Brownian diffusion) BL is completely imbedded within the momentum (or heat) transfer BL, the thickness ratio being proportional to $Sc^{-1/3}$ (or $Le^{+1/3}$). In fact, it can be readily shown (ref. 1) that in the presence of "strong" thermophoresis (i.e., $\alpha_T [(T_e/T_w) - 1] \gg 1$) the Brownian diffusion BL is even much thinner than in the absence of thermophoresis, with the thickness ratio scaling becoming proportional to Sc^{-1} (or Le^{+1}). These observations imply that a finite-difference scheme with a much finer mesh size is required for an accurate solution of the small particle concentration profile and the associated mass transfer Stanton number. Moreover, to preserve accuracy for a two-dimensional integration process, a thinner BL requires a smaller step-size in the x-direction -- i.e., x-direction step-size is restricted by the smallest of the momentum, heat and mass transfer BL thicknesses. Consequently, a moderate increase in the particle size (via Sc) increases the computation time dramatically. In order to achieve a reasonable balance between (a) sufficient thermophoretic deposition rate enhancement (to test the accuracy of our correlations) and (b) required computation time, we have therefore adopted a Schmidt number of about 26 for most of our trials (except for one case with $Sc = 100$, see "Results and Discussion"). Accordingly, the dimensioning of STAN5 has been increased up to 1000 mesh points in the y-direction (from the originally programmed maximum of 60 mesh points)[4].

RESULTS AND DISCUSSION

For all results presented here a mainstream velocity distribution obtained from reference 15 for a turbine stator blade is used as input to STAN5. Except for figure 6, the nose radius, R_n, of the blade used for the illustrative calculations was taken to be 0.152 cm. Integrations were carried out along the suction surface up to about 10 nose radii from the blade stagnation point. In these cases the predicted BL flow remained laminar. To examine the consequence of transition to turbulence (by $x/R_n \approx 5$), for figure 6 the blade was magnified to $R_n = 0.366$ cm and the stagnation pressure was increased from 4 atm. to 20 atm.

In all figures, results at the stagnation point ($x = 0$) are obtained from the self-similar solutions of reference 1 (because STAN5 is singular at x = 0). STAN5 calculations are started at $x = 10^{-1} R_n$. Downstream results are very sensitive to the initial starting profile specified (see also

---

[4]For the fastest commercially available computer, CRAY-1, using 800 mesh points in the y-direction and taking the step-size along the x-direction to be 10^{-1} times the local momentum BL thickness, integration of LBL equations by STAN5 along the suction surface of a typical turbine blade to about 10 nose radii downstream from the stagnation point required a CPU time of about 8 minutes with thermophoresis and 4 minutes without thermophoresis.

ref. 16). To be on the safe side, only STAN5-values beyond one nose radius from the stagnation point were considered reliable (initial profile insensitive). Moreover, by moving one nose radius away from the stagnation point we avoid any anomalities that may result due to (a) lack of accuracy in the mainstream velocity near the stagnation point (ref. 15), and (b) an unrealistic curve-fit generated by the cubic splines that STAN5 employs (ref. 17). The automatic starting profile generating subroutine of STAN5 (ref. 16) was used for the initial velocity and temperature profiles, and the velocity profile was scaled (via $Sc^{-1/3}$) to obtain the initial concentration profile.

The correlation values shown in all figures (with negligible viscous dissipation) are calculated from (refs. 6 and 7):

$$\frac{St_m}{St_{m,o}} \approx \frac{-(B_m + B_T)}{1 - \exp(B_m + B_T)} \cdot \exp(-Da) \tag{4}$$

where:

$$B_m = \frac{(\rho v)_w}{(\rho u)_e St_{m,o}} \tag{5}$$

$$B_T = -(\alpha_T Le)_w \cdot \frac{St_h}{St_{m,o}} \cdot \frac{T_e - T_w}{T_w} \tag{6}$$

and:

$$Da = (\alpha_T Le)_e \cdot \frac{T_e - T_m}{T_m} \tag{7}$$

The Schmidt numbers reported in the figures correspond to particles (assumed spherical) made up of Na_2SO_4 "monomer units" in air[5]. The ratio $\alpha_T Le$ (of the thermophoretic diffusivity of the particles to the heat diffusivity of air), required for our correlations (ref. 6) was estimated to be 0.4 and temperature-independent for all reported cases here. For simplicity in the correlation scheme, throughout this paper the ratio: $St_h/St_{m,o}$, of the Stanton number for heat transfer to the Stanton number for mass transfer without thermophoresis, was approximated to be equal to the prevailing value of $Le_w^{-2/3}$ for laminar BL flows. However, for transitional and fully turbulent flows, local St_h and $St_{m,o}$ values (as calculated by STAN5) are used for the correlation calculations.

To "calibrate" STAN5, we first ran the case of a flat plate (constant mainstream velocity), with the results shown in figure 1. The abscissa is the distance along the flat plate made nondimensional by the stator nose radius $R_n = 0.152$ cm to allow comparisons with the abovementioned turbine blade example. The ordinate is the ratio of mass transfer Stanton numbers

_____

[5]$Sc_\infty = 26$ corresponds to 10^2 and $Sc = 100$ corresponds to 8×10^2 Na_2SO_4 monomer units in a cluster.

(obtained with thermophoresis and without thermophoresis, respectively).
Under the prevailing conditions there is more than a two-fold enhancement in
the deposition rate due to thermophoresis. For this "self-similar" case the
result obtained from the exact numerical calculations of reference 1 is shown
by the dash-dot line (x-independent). The correlation-predicted value is the
dashed line. The only difference between the results of reference 1 and STAN5
should be that due to the somewhat different treatment of variable host gas
(air) thermodynamic and particle transport properties for this "cold" wall
($T_w/T_\infty = 0.6$) self-similar case[6]. However, in interpreting subsequent
comparisons, the reader should recall that STAN5 does not quite give a
constant (x-independent) enhancement.

Figure 2 displays the results of calculations for the suction surface of
a stator blade, using the same environmental conditions as in figure 1. For
the prevailing conditions the Mach number is calculated to be about $Ma_e = 0.72$ at $x/R_n = 10$ (less for smaller x/R_n). To display the effect of
the Mach number STAN5 was also run including viscous dissipation. As expected
(ref. 4), at these Mach numbers viscous dissipation is seen to have a small
effect on the thermophoretic enhancement of deposition rates. Comparison of
our correlations with STAN5 both with and without viscous dissipation shows
that the local difference is always less than 10 percent. The shape of the
curves (i.e., the fact that the effect of thermophoresis decreases as x/R_n
increases) can be explained by the mainstream static temperature cooling.
Although T_w/T_∞ is fixed for our calculations, the difference between
the mainstream static temperature, T_e (which gets cooler as the flow
accelerates under adiabatic conditions), and the wall temperature, T_w
(constant), gets smaller, which reduces the effect of thermophoresis. Of
course, our correlations are also applied locally, with the relevant local
temperature being T_e rather than T_∞.

Figure 3 is constructed for the same conditions as figure 2 except that
the wall temperature is higher ($T_w/T_\infty = 0.8$), corresponding to a smaller
enhancement in deposition rate due to thermophoresis. The agreement between
the predictions of STAN5 and our correlations is excellent.

In figure 4 an increased particle size is considered ($Sc_\infty = 100$),
keeping all remaining parameters the same as in figure 3. The corresponding
effect of thermophoresis is now even greater than in the colder wall case
($T_w/T_\infty = 0.6$) with $Sc_\infty = 26$ (shown earlier in fig. 2). Yet, the
agreement between our correlations and STAN5-predictions is even better, with
local differences being less than 4 percent for all x/R_n-values. This may
be related to our observation (ref. 6) that for self-similar cases these
correlations improve as $T_w/T_\infty \rightarrow 1$, regardless of particle size (Sc).

To consider even larger departures from self-similarity a variable
(x-dependent) wall temperature was considered, with the results shown in
figure 5. T_w is varied in such a way that the wall is hottest at the
stagnation point ($T_w/T_\infty = 0.8$) and gets colder as x/R_n increases,
becoming $T_w/T_\infty = 0.5$ at $x/R_n = 10$. Not surprisingly, the
thermophoretic effect increases as the wall gets cooler (although the

---

[6]Reference 1 assumes that the host gas thermodynamic and particle
transport properties have simple power-law temperature dependencies.

mainstream static temperature drops as the flow accelerates, the reduction in the assumed wall temperature is greater, resulting in a steeper temperature gradient across the BL). While departures between the correlation and STAN5-predictions increase as the wall-to-mainstream-temperature ratio departs from unity (ref. 16), remarkably enough, the effects due to "nonself-similarity" act in such a way that the agreement between STAN5 and the correlations improve as T_w drops.

In figure 6 the nose radius of the stator blade and the pressure have been increased to 0.366 cm and 20 atm, respectively. The corresponding BL flow becomes transitional at about $x/R_n = 2.9$ and "fully" turbulent at about $x/R_n = 5.0$. A lower wall temperature ($T_w/T_\infty = 0.5$) is considered to provide a stringent test of the present correlations, based (ref. 6) on self-similar integrations for $T_w/T_\infty \geq 0.5$. We observe that the agreement between STAN5 and our correlations improves for turbulent BLs. In this connection it should be recalled that our correlations describe the results of law-of-the-wall Couette-flow TBL integrations with even better accuracy than in otherwise corresponding LBL situations. When compared locally with STAN5 results, even for $T_w/T_\infty = 0.5$, agreement is within 10 percent for the laminar portion, and within 4 percent for the fully turbulent portion of the flow. The agreement is still better in the transitional region. Note that the effect of thermophoresis on mass transfer (over and above the already efficient transfer mechanism by turbulent eddies) is smaller than in the corresponding laminar BL case.

Figure 7 displays the results of our calculations on the effect of transpiration cooling and/or thermophoresis on the deposition rate of small particles ($Sc_\infty = 26$). For this purpose STAN5 was run with the wall boundary condition specified as a flux (instead of a level), where the reservoir temperature of the coolant air was taken to be 600K ($T_0/T_\infty = 0.4$). The correlation curve without thermophoresis is representative of how the blowing rate was varied along the blade surface. The blowing rate was set higher near the stagnation point, was reduced along the suction surface, and near the trailing edge ($7 \leq x/R_n \leq 10$) was chosen such that the real blowing parameter, B_m (defined by eq. (5)), was constant.

If attention is first focused on the STAN5 and correlation curves without thermophoresis, observe that STAN5-predictions "lag" in responding to local blowing rate variations when compared with the correlation (which is based on an "instant" assumed adjustment to the local blowing rate). Specifically, for $7 \leq x/R_n \leq 10$, although the correlation predicts a constant reduction in the deposition rate, STAN5-values steadily increase, ultimately approaching the correlation prediction, but remaining below them due to "recollection" of the "history" of higher upstream blowing rates. For a two-dimensional developing BL each x-integration station provides the starting profile for the next station in the forward "marching" process. Therefore, the flow cannot instantaneously adapt itself to the "new" (continuously varying) boundary conditions. A better example is provided if the cross-over points of the curves with and without thermophoresis are compared for the correlation ($x/R_n \approx 7.4$) and STAN5 ($x/R_n \approx 8.2$). Because of mainstream static temperature cooling and the small blowing rates used in this example, the wall temperature becomes hotter than the mainstream static temperature at about $x/R_n \approx 7.4$. Although thermophoresis enhances small particles deposition rates toward colder walls ("suction" effect, ref. 6), for hot walls the

8

deposition rate is <u>reduced</u> due to what we have called "thermophoretic blowing." The correlation curve with thermophoresis, of course, exhibits an immediate reaction to the hotter wall, and crosses the correlation curve without thermophoresis at $x/R_n \approx 7.4$ ($T_w/T_e = 1$). However, STAN5-with thermophoresis responds to the change to a hotter wall further downstream at $x \approx 8.2$ and predicts lower deposition rates than STAN5 - without thermophoresis from then on. We estimate the "lag" in the reaction of STAN5 to be about 9 to 10 local momentum BL thickness for the conditions investigated here. For a blowing rate distribution with more abrupt changes we can therefore expect even larger local disparities between STAN5-predictions and such cor- relations. However, in such cases (with sharp boundary condition variations) it should be recalled that the reliability of STAN5 results themselves becomes questionable[7]. Considering the cost and accuracy features of both methods, the comparisons shown in figure 7 suggest that local applications of our cor- relations will be satisfactory for most engineering design predictions on transpiration-cooled objects.

CONCLUDING REMARKS

To examine the behavior and accuracy of our recently proposed $St_m/St_{m,o}$-correlations of particle mass transport (ref. 6) when applied locally to developing GT-boundary layer situations, we have embarked on a program of selected numerical computations and controlled laboratory experiments (ref. 5). Progress in the former category is reported here, and in view of the widespread familiarity and use of the two-dimensional BL code STAN5 (ref. 11 and 9) for GT <u>heat</u> transfer predictions, we have described how STAN5 has been adapted for mass transfer (deposition) rate predictions for cooled combustion turbine blades. Most importantly, the program has been modified to include thermal (Soret) diffusion ("thermophoresis" for small particles) in the suspended particle mass conservation equation. The transport properties (i.e., Brownian diffusion coefficient, thermal diffusion factor) of small particles (considered simply as "heavy molecules") are calculated allowing for their variation with temperature across the boundary layer. The program dimensioning is increased to accurately obtain the sus- pended particle concentration profile inside the much "thinner" (cf., thermal and momentum boundary layer thickness) mass transfer (Brownian diffusion) boundary layer for small particles ($Sc \gg 1$).

STAN5 predictions of mass transfer coefficients are then used to examine the behavior and accuracy of correlations we recently developed to predict the enhancement in deposition rates due to thermophoresis in the presence of variable properties, transpiration cooling and/or viscous dissipation. These correlations, which successfully described results for self-similar <u>laminar</u> boundary layers, and law-of-the-wall <u>turbulent</u> boundary layers (ref. 6), are here found to be quite satisfactory and very economical, when applied <u>locally</u> to developing laminar and turbulent high Schmidt number mass transfer boundary layers.

Whatever is projected for electronic computational capabilities, more realistic system predictions/optimizations will inevitably require subroutines

---

[7]See reference 18 for a comparison of STAN5 predictions with experimental <u>heat</u> transfer around a gas film-cooled cylinder in cross-flow.

which <u>economically</u> incorporate the results of prior BL integrations. In view of the complexity and the often <u>prohibitive</u> cost of running repetitive PDE simulations for day-to-day engineering design calculations, the comparisons discussed here suggest that local application of our previous mass transfer correlations (ref. 6) can cover typical cases of GT-interest with acceptable accuracy.

REFERENCES

1. Gökoğlu, S. A. and Rosner, D. E., "Thermophoretically-Augmented Forced Convection Mass Transfer Rates to Solid Walls Across Non-Isothermal Laminar Boundary Layers," <u>AIAA Journal</u>, (submitted, 1983).

2. Gökoğlu, S. A. and Rosner, D. E., "Effect of Particulate Thermophoresis in Reducing the Fouling Rate Advantages of Effusion-Cooling," <u>International Journal of Heat and Fluid Flow</u>, vol. 5, no. 1, Mar. 1984, pp. 37-41,.

3. Gökoğlu, S. A. and Rosner, D. E., "Thermophoretically Enhanced Mass Transport Rates to Solid and Transpiration-Cooled Walls Across Turbulent (Law-of-the-Wall) Boundary Layers," <u>Industrial and Engineering Chemistry -Fundamentals</u> (in press, 1984).

4. Gökoğlu, S. A. and Rosner, D. E., "Viscous Dissipation Effects on Thermophoretically-Augmented Particle Transport Across Laminar Boundary Layers," <u>International Journal of Heat and Mass Transfer</u> (in press, 1984).

5. Rosner, D. E. and Kim, S. S., "Optical Experiments on Thermophoretically Augmented Submicron Particle Deposition from 'Dusty' High Temperature Gas Flows," <u>Chemical Engineering Journal</u> (Lausanne), vol. 28, (in press, 1984).

6. Gökoğlu, S. A. and Rosner, D. E. "Correlation of Thermophoretically-Modified Small Particle Diffusional Deposition Rates in Forced Convection Systems with Variable Properties, Transpiration Cooling and/or Viscous Dissipation," <u>International Journal of Heat and Mass Transfer</u> vol. 27, no. 5, 1984, pp. 639-645,.

7. Rosner, D. E., Gökoğlu, S. A. and Israel, R., "Rational Engineering Correlations of Diffusional and Inertial Particle Deposition Behavior in Non-Isothermal Forced Convection Environments," <u>Fouling of Heat Exchange Surfaces</u>, Engineering Foundation, New York, 1983, pp. 235-256.

8. Cebeci, T., Smith, A. M. O., and Wang, L. C., "A Finite-Difference Method for Calculating Compressible Laminar and Turbulent Boundary Layers, Part I," Report No. DAC-67131, McDonnell-Douglas Co., Aircraft Div., St. Louis, MO, Mar., 1969.

9. Patankar, S. V. and Spalding, D. B., <u>Heat and Mass Transfer in Boundary Layers: A General Calculation Procedure</u>, 2nd Ed., Intertext, London, 1970.

10. Mengütürk, M. and Sverdrup, E. F., "A Theory for Fine Particle Deposition in Two-Dimensional Boundary Layer Flows and Application to Gas Turbines," <u>Journal of Engineering for Power</u>, vol. 104, no. 1, Jan. 1982, pp. 69-76.

11. Crawford, M. E. and Kays, W. M., "STAN5 -- A Program for Numerical Computation of Two-Dimensional Internal and External Boundary Layer Flows," NASA CR-2742, 1976.

12. Rosner, D. E. and Fernandez de la Mora, J., "Small Particle Transport Across Turbulent Nonisothermal Boundary Layers," <u>Journal of Engineering for Power</u>, vol. 104, no. 4, Oct. 1982, pp. 885-894.

13. Fernandez de la Mora, J., "Deterministic and Diffusive Mass Transfer Mechanisms in the Capture of Vapors and Particles," Ph.D. Dissertation. Yale University, 1980.

14. Gökoğlu, S. A., "Thermophoretically Enhanced Deposition of Particulate Matter Across Nonisothermal Boundary Layers," Ph.D. Dissertation, Yale University, 1982.

15. Haas, J. E. and Kofskey, M. G., "Cold-Air Performance of a 12.766-Centimeter-Tip-Diameter Axial-Flow Cooled Turbine II-Effect of Air Ejection on Turbine Performance," NASA TP-1018, 1977.

16. Gaugler, R. E., "Some Modifications to, and Operational Experiences with, the Two-Dimensional, Finite-Difference, Boundary-Layer Code, STAN5," NASA TM-81631, 1981.

17. McCartin, B. J., "Applications of Exponential Splines in Computational Fluid Dynamics," AIAA Journal, vol. 21, no. 8, Aug., 1983, pp. 1059-1065.

18. Stepka, F. S. and Gaugler, R. E., "Comparison of Predicted and Experimental External Heat Transfer Around a Film Cooled Cylinder in Crossflow," ASME Paper 83-GT-47, 1983.
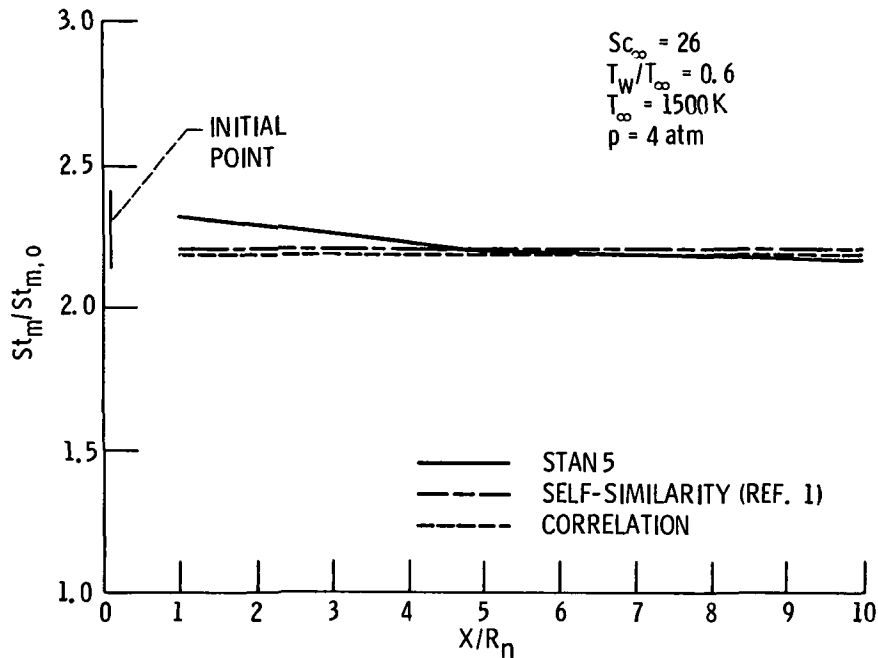
FIG. 1 Accuracy of STAN 5 [11] and correlations [6,7] in predicting
the thermophoretic enhancement of particulate mass transfer rates
when compared to self-similar laminar boundary layer calculations
[1] for a flat plate; $Sc_\infty = 26$, $T_w/T_\infty = 0.6$.
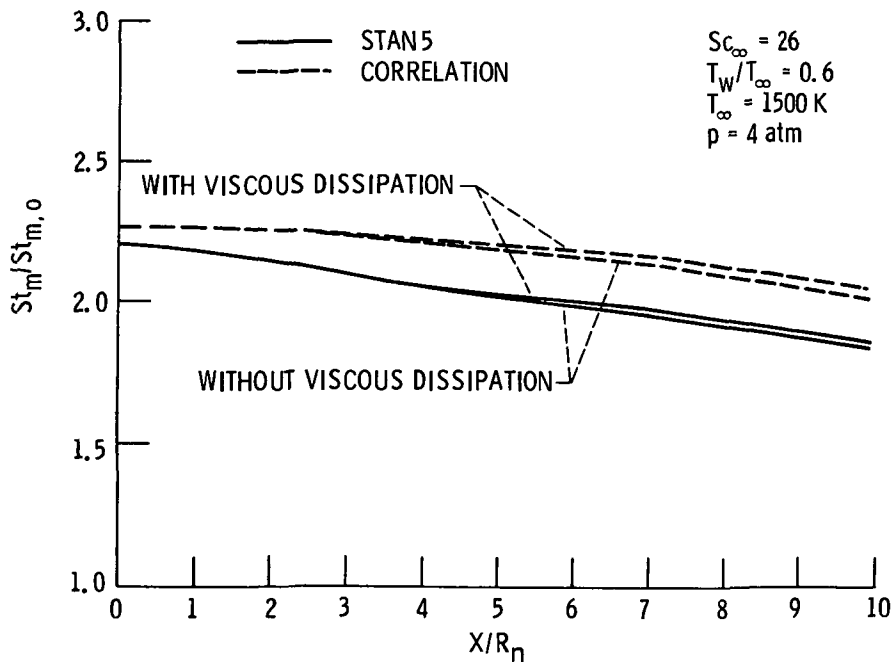
FIG. 2 Comparison of correlations [6,7] with STAN 5 [11] predictions
of mass transfer rate enhancement due to thermophoresis both with
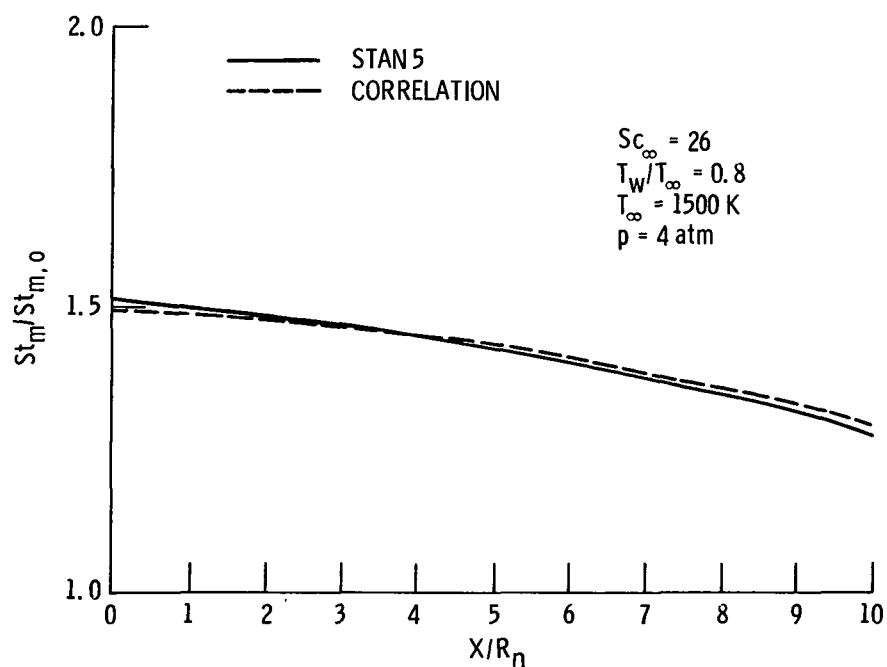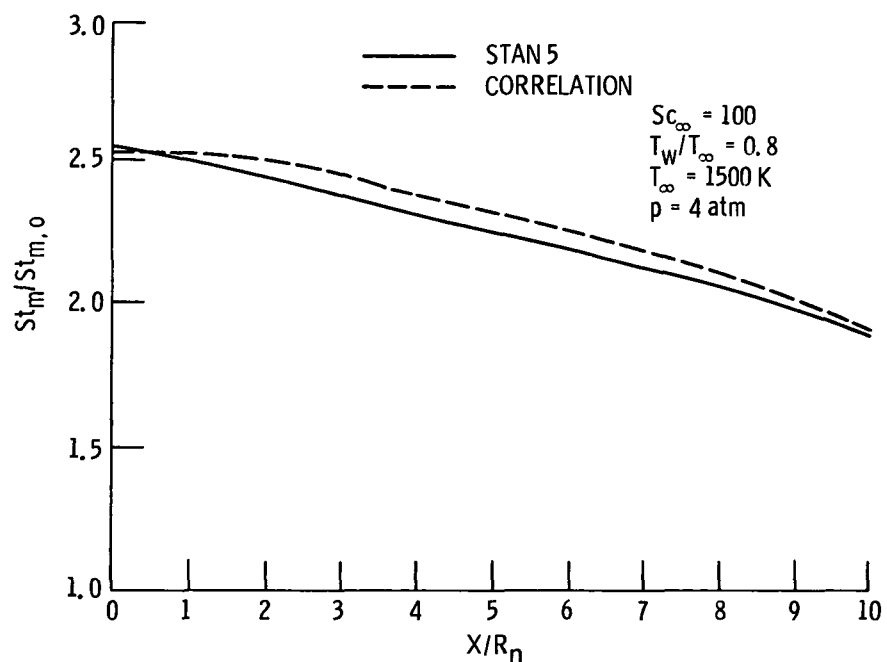and without viscous dissipation; GT stator [15], $Sc_\infty = 26$, $T_w/T_\infty = 0.6$.

FIG. 3 Comparison of correlations [6,7] with STAN 5 [11] predictions of mass transfer rate enhancement due to thermophoresis; GT stator [15], $Sc_\infty = 26$, $T_W/T_\infty = 0.8$.

FIG. 4 Comparison of correlations [6,7] with STAN 5 [11] predictions of mass transfer rate enhancement due to thermophoresis; GT stator [15], $Sc_\infty = 100$, $T_W/T_\infty = 0.8$.
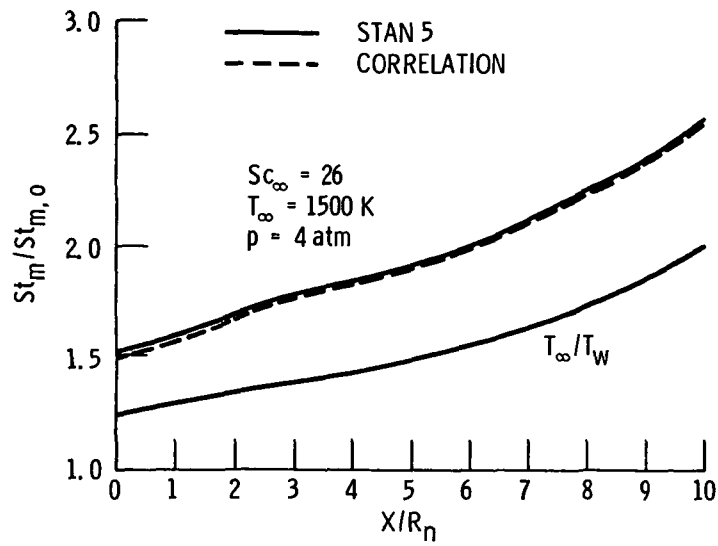
FIG. 5 Comparison of correlations [6, 7] with STAN 5
[11] predictions of mass transfer rate enhancement
due to thermophoresis for a variable wall tempera-
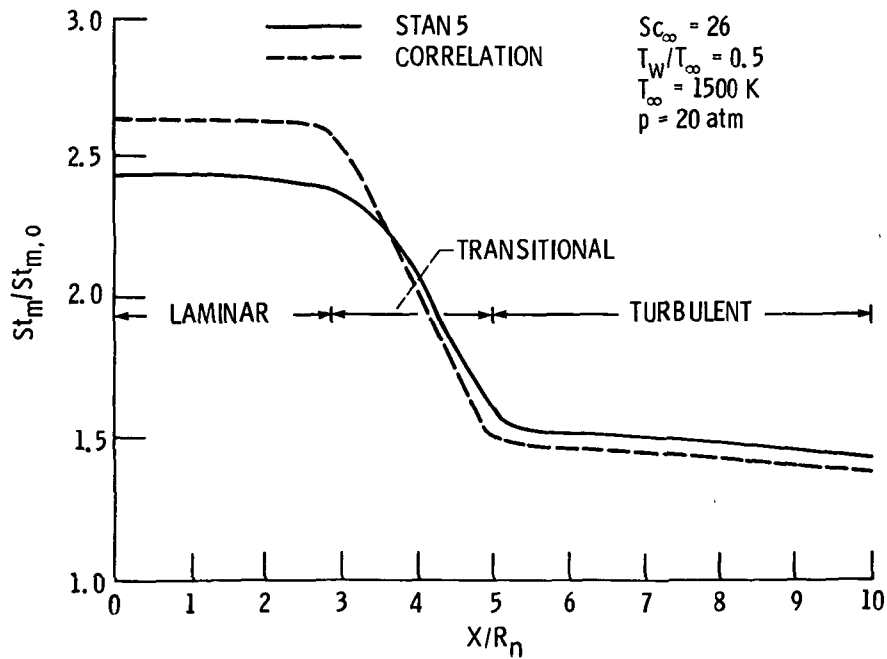ture, GT stator [15] (T_w/T_∞ = 0.8 ⟶ 0.5).

FIG. 6 Comparison of correlations [6, 7] with STAN 5 [11] predictions
of mass transfer rate enhancement due to thermophoresis allowing
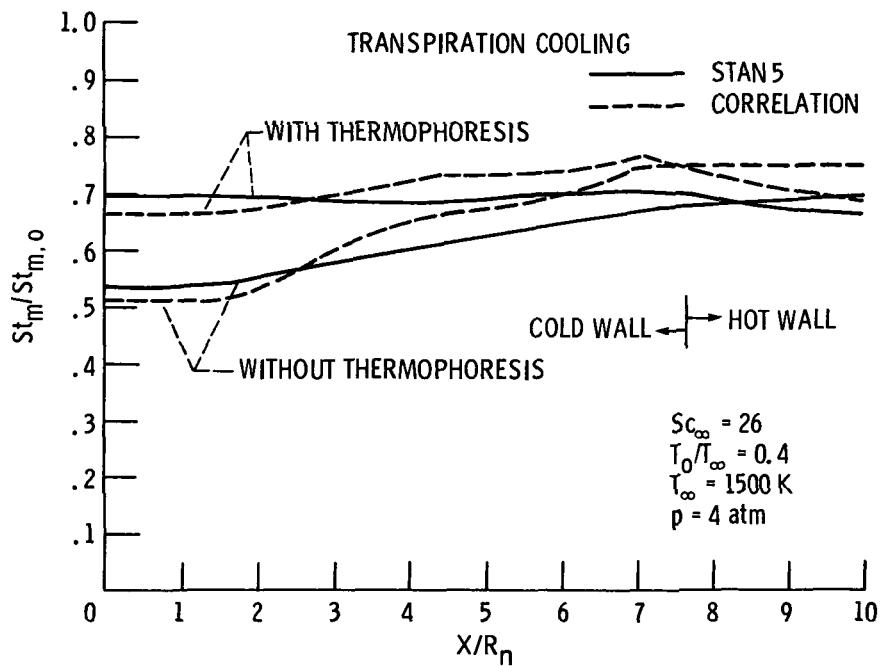transition to turbulence; GT stator [15], Sc_∞ = 26, T_w/T_∞ = 0.5.

FIG. 7 Comparison of correlations [6, 7] with STAN 5 [11] predictions
of mass transfer rate reductions in the presence of gas transpiration
cooling, both with and without thermophoresis; GT stator [15],
$Sc_\infty = 26$, $T_0/T_\infty = 0.4$.

1. Report No. NASA CR-168221	2. Government Accession No.	3 Recipient's Catalog No
4 Title and Subtitle Comparisons of Rational Engineering Correlations of Thermophoretically-Augmented Particle Mass Transfer with STAN5-Predictions for Developing Boundary Layers		5 Report Date January 1984
		6 Performing Organization Code
7. Author(s) Süleyman A. Gökoğlu and Daniel E. Rosner		8 Performing Organization Report No None
		10 Work Unit No
9. Performing Organization Name and Address Analex Corporation and Yale University 21000 Brookpark Rd. Chemical Engineering Dept. Cleveland, Ohio 44135 New Haven, Connecticut 06520		11 Contract or Grant No NAS3-23293 and NAG3-201
		13 Type of Report and Period Covered Contractor Report
12. Sponsoring Agency Name and Address National Aeronautics and Space Administration Washington, D.C. 20546		14 Sponsoring Agency Code 533-04-1A (E-1991)

16. Abstract

Fouling (and corrosion) of gas turbine (GT) blading often results from the deposition of materials derived from inorganic impurities in the fuel and/or ingested air. When the depositing material is in the form of a submicron "aerosol" (dust or mist) it has been found that the rates of deposition on cooled surfaces can be augmented by some 100-1000-fold via the mechanism of thermophoresis (particle migration down a temperature gradient). For this reason, in earlier papers we reported the development of rational, yet simple, engineering correlations of thermophoretically-augmented particle transport across both laminar boundary layers (LBLs) and turbulent boundary layers (TBLs). While developed based on theoretical considerations, and numerical computations of self-similar LBLs and law-of-the-wall (Couette flow-like) TBLs, these mass transfer coefficient (St_m-) correlations, when applied locally, may also prove useful in making engineering mass transfer predictions for more complex geometries, including GT-blades. Pending additional controlled experiments, insight into the local applicability of these correlations can be gained by selected comparisons with numerical predictions for developing BLs. This paper reports on our (a) modification of the code STAN5 to properly include thermophoretic mass transport, and (b) examination of selected test cases developing BLs which include variable properties, viscous dissipation, transition to turbulence and transpiration cooling. Under conditions representative of current and projected GT operation, local application of our $St_m/St_{m,0}$- correlations evidently provides accurate and economical engineering design predictions, especially for suspended particles characterized by Schmidt numbers outside of the heavy vapor range (say, $Sc > 10$).

17. Key Words (Suggested by Author(s)) Deposition; Boundary layer; Thermophoresis; Corrosion; Mass transfer; Gas turbine	18. Distribution Statement Unclassified - unlimited STAR Category 31

19. Security Classif. (of this report) Unclassified	20. Security Classif. (of this page) Unclassified	21. No. of pages	22. Price*

National Aeronautics and
Space Administration

Washington, D.C.
20546

SPECIAL FOURTH CLASS MAIL
BOOK

NASA

POSTMASTER: If Undeliverable (Section 158
Postal Manual) Do Not Return